Astrocyte-Neuron co-cultured 3D tumor spheroid model for Anti-cancer Drug Screening

Sivasubramanian Murugappan[1], Ajay K. Mali[1], Syed A. M. Tofail[1,2]

Nanasaheb D. Thorat[1,2,]*

[1]Department of Physics and Bernal Institute, University of Limerick, Castletroy, Limerick V94T9PX, Ireland

[2]Limerick Digital Cancer Research Centre (LDCRC), University of Limerick, Castletroy, Limerick V94T9PX, Ireland

[*] - Corresponding Author: nanasaheb.d.thorat@ul.ie

ABSTRACT

Previous literature has strongly established the close relation between astrocyte and neuron communication, how they are interdependent and can't function properly without their counterpart's presence. Still, pre-clinical studies are done in 2D monocultures which do not reciprocate *in vivo* or animal models which don't exactly mimic the human tumor microenvironment. In this researchwork, we have come up with a co-cultured spheroid model of glioblastoma cells (U87-MG) and neuroblastoma cells (SH-SY5Y). The co-cultured spheroid was grown with controlspheroids (individual U87-MG and SH-SY5Y) for 14 days. Furthermore, the FDA approvedbrain cancer drug, Temozolomide (TMZ) was screened against them. The growth and drug treatment experiments carried out helps in a holistic understanding of the brain tumor reflecting the *in vivo* human tumor microenvironment and to design anti-cancer drugs appropriately. Major takeaways from the study were, Glioblastoma (U87-MG) thrives under hypoxic conditions and is resistant to TMZ even at high concentration of 1000μM, the neuroblastoma (SH-SY5Y) spheroids were sensitive to TMZ and sensitized the co-cultured model for TMZ resulting in significant decrease in cell viability. They also presented strong prospects of being differentiated in the process as they displayed elongated neurite like morphology in 3D.

Keywords: Spheroids, Glioblastoma, Neuroblastoma, Temozolomide, 3D Tumor models.

1. INTRODUCTION

Getting to understand the neuron-glia interaction in the brain is essential to make informed decisions in disease modelling and drug development as the literature has evidently proves their direct and indirect intercellular communication both in normal and disease conditions. In response to brain abnormalities, glial cells exhibit phenotypic changes that can range from proinflammatory and neurotoxic, to anti-inflammatory and neuroprotective, showing their wide plasticity[1]. The Astrocytes play a vital role in arranging the metabolic and spatial support required for neurons. It also performs crucial functions in neuronal differentiation, migration and synaptic activity[2]. Therefore, dysfunction of the astrocytes leads to a cascade of cytotoxic events antagonizing glial-neural networks resulting in neurological disorders. Neurons and astrocytes both have the ability to completely oxidize glucose and lactate, as they both have same number of mitochondria. But they use different yet complementary pathways steering metabolic cooperation for it. While astrocytes demonstrate lower rates of oxidative metabolism in comparison to neurons, they are known for their high glycolytic rate and avid uptake of glucose. Though their energy expenditure constitutes for only 5-15% of the overall energy spent in the brain. This is because a significant amount of this glucose enters the glycolytic pathway of the astrocytes and gets released as lactate in the extracellular region which in turn is used to produce oxidative-derived ATP by the neurons. And this whole model is called the Astrocyte-Neuron Lactate Shuttle (ANLS)[3]. The strong alliance of neuron–neuron synapses to astrocytes aids in stabilizing synaptic connections and the clearance of neurotransmitters. Neuronal activation leads to evident shifts in the intracellular Ca^{2+} concentrations of astrocytes. Similarly, a reduction in the release of neuronal glutamate hinders the maturation of the astrocytes[4]. One major series of communication happening between the neuron-astrocytes is the Glutamine-glutamate-GABA cycle. Astrocytes produce pyruvate carboxylase, the key enzyme to synthesize glutamate from glucose. Neurons release the glutamate or GABA into the synaptic cleft of astrocytes. These astrocytes then enters the TCA cycle through GABA shunt and converts the GABA to Succinyl CoA or the glutamate to glutamine using glutamine synthetase, an astrocyte specific enzyme. This glutamine is sent back to neurons to perform their role as precursors for the synthesis of neurotransmitters[3,5]. Neurons rely on critical functions provided by astrocytes in the healthy central nervous system (CNS). These functions include modulating synapses, maintaining the blood-brain barrier (BBB), supplying trophic and metabolic assistance to neurons[6].Even though neuron performs most of brain's oxidative metabolic activities, they are more prone to oxidative stress than astrocytes. In co-cultures,

astrocytes have been reported to have protected the surrounding neurons in times of oxidative stress or damage. Changes in the optimal level of glutathione (GSH) in astrocytes affected the neurons negatively during oxidative injury as neurons depend on the astrocytes for the precursor amino acids needed to synthesize their own GSH. Astrocytes showcase a higher basal penta-phosphate pathway (PPP) activity rate and has more NADPH compared to neurons[3]. This also stimulates quicker and appropriate retort to oxidative stress. All these factors together strongly display the antioxidant capacity of astrocytes and their protective behavior for neurons. Any small alterations in this widespread functional cooperation of astrocytes and neurons can lead to neuronal dysfunction.

The tumor microenvironment (TME) of the brain plays a major role in the pathogenesis of various brain conditions including neurodegenerative disorders, cancer, epilepsy etc. The factors influencing decisions in the brain TME primarily involve the neurons and glial cells (astrocytes, microglia and oligodendrocytes). The communication between neurons and glial cells is bi-directional. This can be realized during modulations in neuronal activity, pathology and phenotype. Neurons stimulate astrocyte maturation through the exchange of growth factors and cell-cell contact. The transforming growth factor (TGF)-β signal required for astrocyte differentiation is initiated from the mature neurons. Neuronal membrane inhibits astrocyte proliferation actively maintaining homeostasis. Neurons suppress the glioblastoma cells from breaking down the brain parenchyma by limiting the TGF-β and mitogen activated protein kinases establishing themselves as a strong tumor suppressor[7]. With 80% of glioma population reporting seizures during disease, glioma malignancy can be attributed as a common cause for epilepsy. These patients displayed over 200-fold increase in glutamate concentrations than normal cerebrospinal fluid levels. In astrocytoma, it has been reported that instead of exhibiting inhibitory GABA response, peritumoral neurons and tissues showed hyperexcitability[8]. Similar results were observed in a cell-insert co-culture system of hippocampal neurons revealed that 90% of βIII -Tubulin positive cells expressed VGLUT and only the remaining 10% constituted for GABA making the neurons majorly highly excitatory and minimally inhibitory[9]. Primary brain tumors are enriched with matrix-degrading enzymes. Their invasion and progression are influenced by the digestion and remodeling of the extracellular matrix (ECM), including chondroitin sulfate proteoglycans (CSPGs).

Reactive astrocytes are known to inhibit neurite outgrowth by secreting CSPGs[8]. The migration of new neurons is suppressed by the dense mesh of astrocytes and neurons. The CSPGs synthesized by astrocytes fill the mesh and restrict glioma cell invasion by forming a mechanical barrier. Contradictory data have also been reported suggesting CSPGs enhance glioma migration and cell adhesion[7]. High levels of tumor derived astrocytic factors like that of thrombospondin-1 often seen in IDH-WT glioblastoma, being well connected to neuronal network influences patient survival by remodeling synaptic connections in the brain TME. In Glioma cells, not only the production of synaptogenic factors and neurotransmitters but also secretion of glutamate and selected point mutations in *PIK3CA* gene of glioblastoma drive neuronal hyperexcitability which in turn have led to epileptic activity. Both primary and metastatic brain tumor cells showed enhanced stemness, proliferation and resistance to therapy when grown under astrocyte conditioned media. Glioblastoma associated astrocytes displayed an anti-inflammatory shape and hyperactivity of the JAK/STAT modifying the immune microenvironment to promote metastasis. The gap junction coupling in tumor- tumor networks formed by both pediatric and adult glioma cells like normal astrocytes, direct calcium (Ca) transients to get inline upon neuronal activation in glioma cells. These astrocytes secrete inflammatory cytokines in response to the delivery of cGAMP, a secondary messenger by the metastatic cells of the brain supporting the chemoresistance and growth of cancer cells[4].

Preclinical research requires disease models that work towards minimizing the use of animals in investigatory and regulatory vivo studies. To get this done, the models developed should follow the fundamental 3R principles (replacement, reduction and refinement). Also, apart from the ethical concerns, animal models cannot be considered for mimicking the in vivo environment of human brain as they don't reflect it. Astrocytes in the human brain are larger and high in number with 10 times more brain activity than rodent brain. Unique varicose projections, interlaminarity are all present only in human astrocytes[2]. Though organoid models show great promise, they require longer maturation periods usually a couple of months minimum. Also, they lack the precise ratio of neurons to glial cells let alone astrocytes[10]. Among pre-clinical studies, over 66% use 2D cell culture while 3D cell culture contributes for only 10%. 2D cell culture are well established,

reproducible and easy to perform but they lack the purpose of reflecting human environment. Hence, an easy, reproducible yet working model is required. Multi-cellular tumor spheroids (MCTS) are the solution for that. MCTS are tightly packed self-assembled cultures of tumor cells which closely reflect the *in vivo* tumor architecture of humans. MCTS could produce their own extracellular matrix (ECM) proteins like collagen, glycosaminoglycans, fibronectin and laminin. MCTS formation and compactionis heavily dependent on the integrin-ECM interaction followed by Cadherin-cadherin interactions and type-I collagen levels[11,12]. Herein, we have come up with one such 3D tumor model co-culturing neurons and astrocytes. Spheroids are consistently grown using one of the following techniques Hanging-drop method (HD), Liquid Overlay technique (LOT), Spinner bioreactors, Microfluidics etc. We have opted for the liquid overlay technique due to its high reproducibility, reduced error and variability and ease of handling compared to other methods. In LOT, the well plates are coated with various gels to avoid cell –plate adherence while promoting cell-cell adhesion[13]. In this work, we have used agarose for surface coating because it is soluble only at temperatures of 65°C and above, its inexpensiveness, easy dissolution and sterilization[14].

In this research article we have developed a co-cultured multicellular tumor spheroid (MCTS) system combining U-87MG Glioblastoma cell line and SH-SY5Y Neuroblastoma cell line in a simple straightforward single step Gel-embedding method to better understand brain tumors and their targeted drugs.

2. RESULTS

2.1 SPHEROID GROWTH

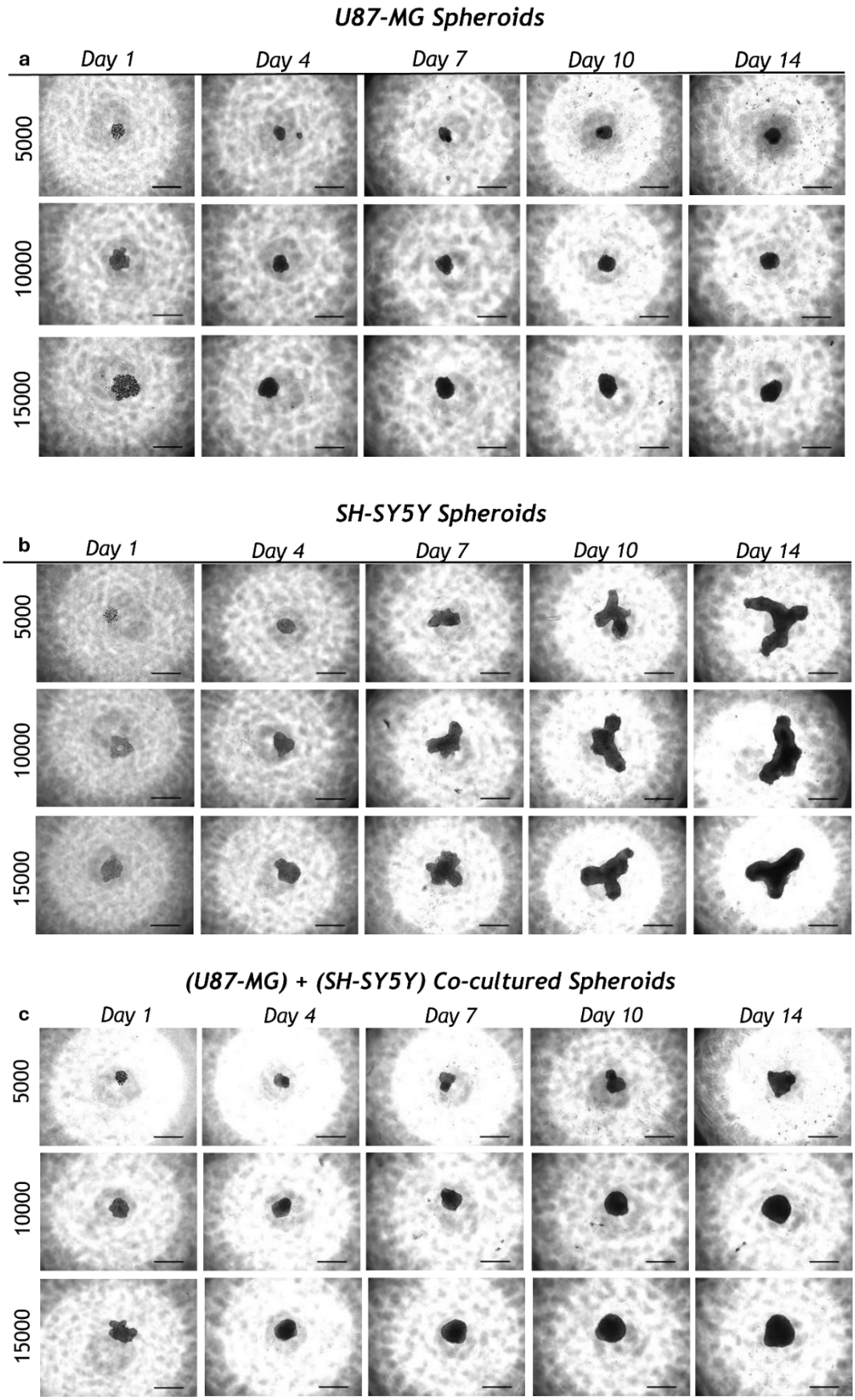

Figure 2.1.1 Spheroid growth over 14 days with cell seeding densities of 5000,10000 and 15000 cells: U87-MG (a), SH-SY5Y (b) and co-cultured spheroid (U87-MG)+(SH-SY5Y))(c). Scale 500μm

The U87-MG spheroids maintained a compact spherical shape in all three different cell densities. The 5k cell group images displayed (Fig 2.1.1a) the ability of cells to have cell-cell communication. It can be noticed that two smaller spheroids formed apart from the main spheroid, moving towards (See supplementary figure S1a for Day 1 to 14 images) the main spheroid and getting fused with them. Similar cell-cell communication was observed on 10k group as well, on the initial 3 days (See supplementary figure S1b for Day 1 to 14 images), after which they merged to form a single spheroid. The 14th day image implies only the formation of a dense hypoxic region. This holds true as the size of the spheroids with 5k and 10k cells for different sets remained at around ~400µm and ~500µm respectively at the end of 14 days. Literature studies suggested that only spheroids of size above ~500µm show necrotic core[15]. Necrotic core was visible in the 15k group on the last couple of days in the 14-day period. And rightfully, their sizes were above ~500µm at about ~600µm. The U87-MG glioblastoma spheroids have been consistent in their growth showing slow and gradual linearity in terms of increase in their area (Fig 2.1.1a).

For the neuroblastoma spheroids formed from SH-SY5Y cell line, all three spheroid groups followed an irregular but identical elongated pattern. The growth morphology observed is close to that of neurite protrusions in neurons following a pyramidal neuronal architecture which strongly branches out with a central core. During the initial days, they developed the core and around the 7th day (earlier in case of highest density 15k cells) they started to branch out in different directions. In the case of 15k cells, even when they protruded in another direction on Day 11, they fused back (Day 12) to form the tripolar pyramidal neuronal structure (See supplementary figure S2c). All three cell densities started showing hypoxic regions from Day 9. The hypoxic regions were majorly seen in the node points from where the neurite like protrusions began. On Day 14, evident necrotic regions were observed in 10k and 15k cell groups (Fig 2.1.1 b) in the same hypoxic region found on Day 9 clearly depicting hypoxia leads to necrosis in neuroblastoma. It is important to note the initial couple of days of growth in 10k cells density group, they had formed into a dough nut shaped spheroid. This was also faintly visible in 15k group of glioblastoma spheroids on the 1st day. In our trial studies testing different cell densities and types as well, this pattern of growth was seen. Hence, we hypothesize that all cells once cultured usually form a doughnut-like pattern irrespective of the cell type and move inward towards center and then grow outward to form the spheroids.

Co-culture spheroids of U87-MG and SH-SY5Y grew at a ratio of 1:1 cell density. The spheroids grew larger than their glioma counterparts. However, they maintained

spherical morphology as displayed by glioma spheroids. The 5k group alone, slightly deviatedfrom the spherical morphology. This could be reasoned for astrocytes to influence their behavior, there might be a minimum threshold of cells required. Unlike the neuroblastoma spheroids which showed strong necrotic core and glioma spheroids which didn't show any necrosis, the co-culture took a middle stand with a small necrotic core compared to neuroblastoma spheroids. This can be attributed to their sizes as they remained consistently above 600µm for all cell densities. But the spherical morphology and area being closer to thatof U87-MG spheroids could be due to the higher proliferation rate of U87-MG cells found in 2D compared toSH-SY5Y, being seen in 3D environment as well [16].

In this work, we have calculated the area of spheroids not the volume, mainly due to irregular shape of neuroblastoma which on visual observations showed longer length and width (see also in Fig 2.1.1b) but the depth was comparatively thinner, and the z-levels ofprotrusions were different. This way of extrapolating to volume or considering 1-D size might notreflect the actual morphology as much as the area measurements.

This growth morphologies of spheroids, may it be spherical shape in glioblastoma and co-cultured spheroid or the neuronal elongations seen in neuroblastoma spheroids indicate the inherent behavior of cells having strong implications on a tissue level. Thus, these morphological understandings are of key importance as they give a sense of direction tounderstanding different spheroid's growth mechanism helping in design better 3D models reflecting the *in vivo* environment.

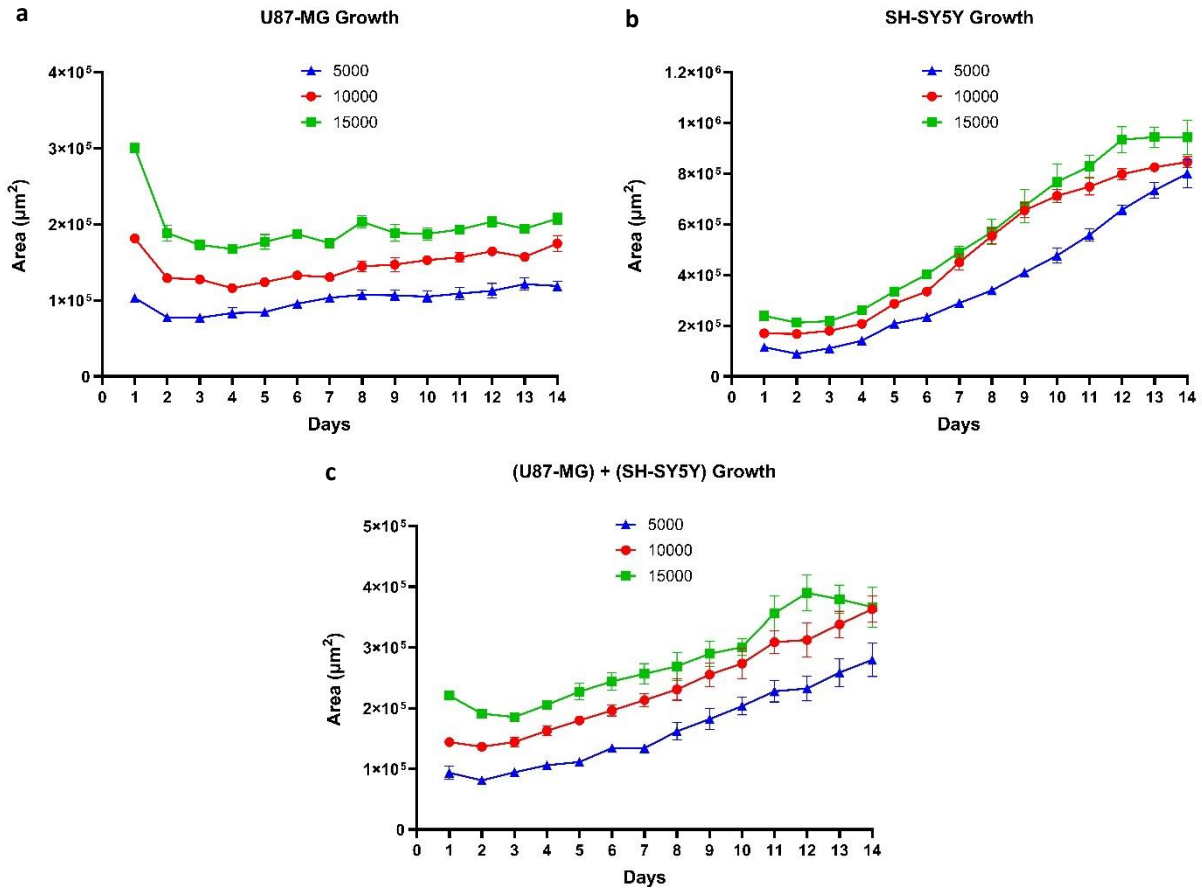

Figure 2.1.2. *Growth Rate of Spheroids: U87-MG (a), SH-SY5Y (b), (U87-MG) +(SH-SY5Y) co-cultured spheroids (c)*

The growth of spheroids over a period of 2 weeks (14 days) has revealed that spheroid growth rate is dependent on cell type (Fig 2.1.2). Still, all the groups discussed had the same pattern of growth irrespective of the type and took about 4 days to form a spheroid. After the initial 4 days, they started growing steadily. The increase in area of U87-MG here was slow compared to SH-SY5Y. The area increases on the co-cultured spheroids remained in between but tending to a slower rate as that of U87-MG. This was quite unexpected as U87-MG has a faster proliferation rate than SH-SY5Y in 2D cell culture. This could be due to irregularity in the shape of SH-SY5Y where the depth was less formed and well contained but loosely aggregated spheroids unlike the U87-MG, which formed tightly packed spheroids. The growth rate of co-culture being higher than but close to U87-MG demonstrates the dominant behavior of glioma at the same time represents the activity of neuronal cells. Some data points on the (Fig 2.1.2a) suddenly sees a spike in area, it is attributed to the media replenishment. The larger area on 8th day in U87-MG could be because of the media replenishment was done on 7th day which in turn led to a faster proliferation of the proliferation zone. This again falls back to the growth pattern expected on 9th day shows compaction of the spheroids is a continuous process visibly seen whenever mitosis overtakes the rate of necrosis. The growth after 10th day in SH-SY5Y and co-culture groups started moving towards attaining a state of saturation. This saturation happens based

on size rather than being time dependent or cell density. Thus U87-MG also would reach the stage, but the timeline required is expected to be longer. This said, based on the cell type a minimum cell density is needed for them to reach saturation. This seems to be lacking with U87-MG cells with an initial cultured cell density of 5000 cells.

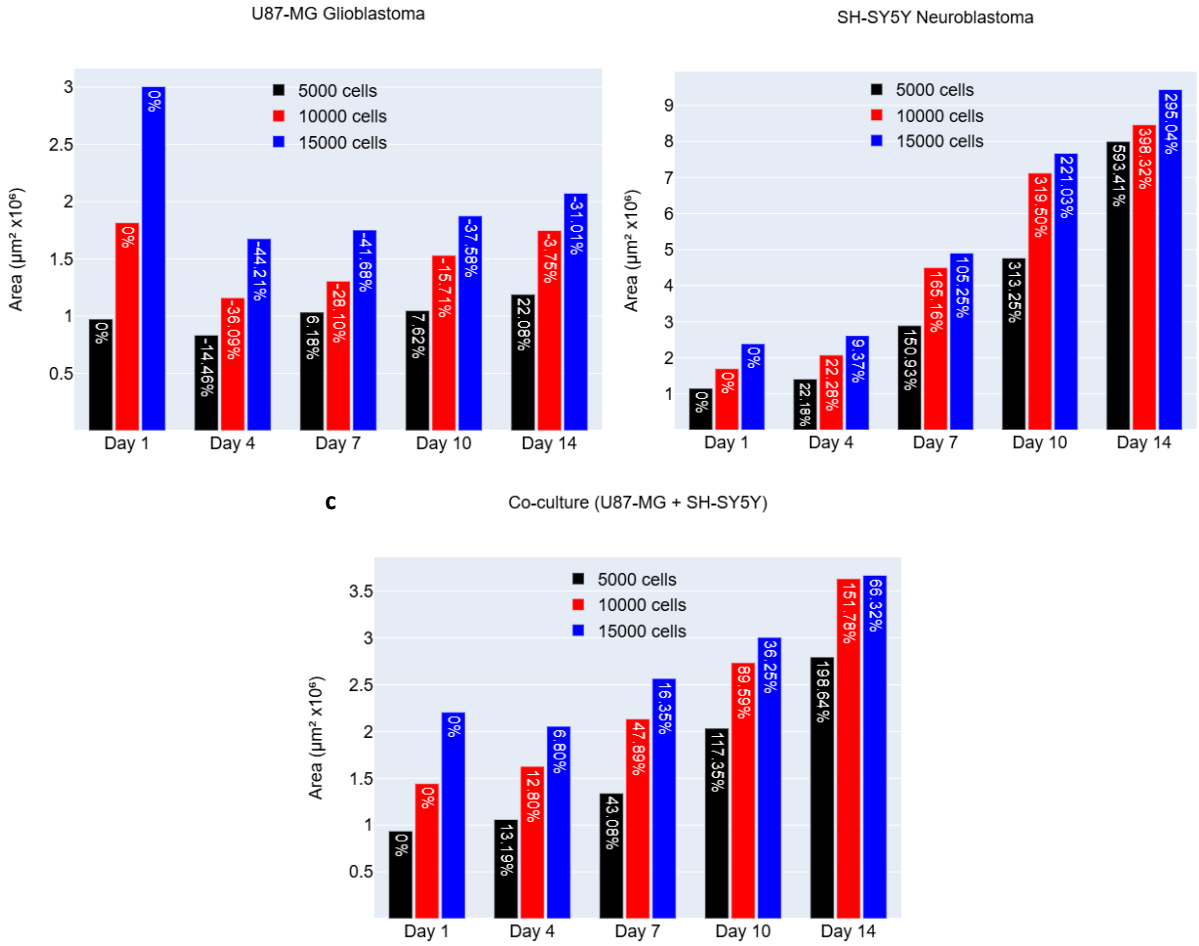

Figure 2.1.3. Spheroid Invasion rate: U87-MG (a), SH-SY5Y (b), (U87-MG)+(SH-SY5Y) co-cultured spheroids (c)

Irrespective of the spheroid group, the lesser the cell density higher was the invasion. The rate of invasion as well, was faster in less dense groups (Fig 2.1.3). This is because, in groups with smaller initial cell density there is more nutrient and oxygen per capita. Likewise, all cells regardless of their type and density undergo compaction between Day 1 and 4 (Supplementary Figure S2). In the co-cultured 3D model, approximately ~66% increase in invasion area was observed in 15k cells while ~150% and ~200% growth was noted in 10k and 5k cells respectively, indicating exponential growth. Over time, it was noticed that higher density cell groups moved towards a size limiting phase sooner compared to other low-density groups. For neuroblastoma, itwas ~300%, ~400% and ~600% for 15k,10k and 5k cells. But this invasion wasn't consistent. Between days 4 and 7, 15k cell's invasion grew by 10 times while 10k and 5k cells grew only by 6 times. But later within Days 7 to 10, they doubled for all cell densities. In the final 10th to 14th day, 15k and 10k grew only by 50% whereas 5k still maintained

the rate and doubled in invasion area. This clearly shows that high dense cells grow at high rates initially but slow down later and the opposite stands true for less dense cells. The glioblastoma group were loosely aggregated till 4 days (Supplementary Figure S1) for all cell densities and started invasion only after. The 15k cells saw an insignificant growth of about 10% over 14 days. 5k and 10k cells showed 40% increased invasion area. This growth, however not significant to the levels of neuroblastoma and co-cultured spheroids, the pattern holds true with high cell density groups invading slowly than theless dense ones.

2.2 LIVE DEAD ASSAY

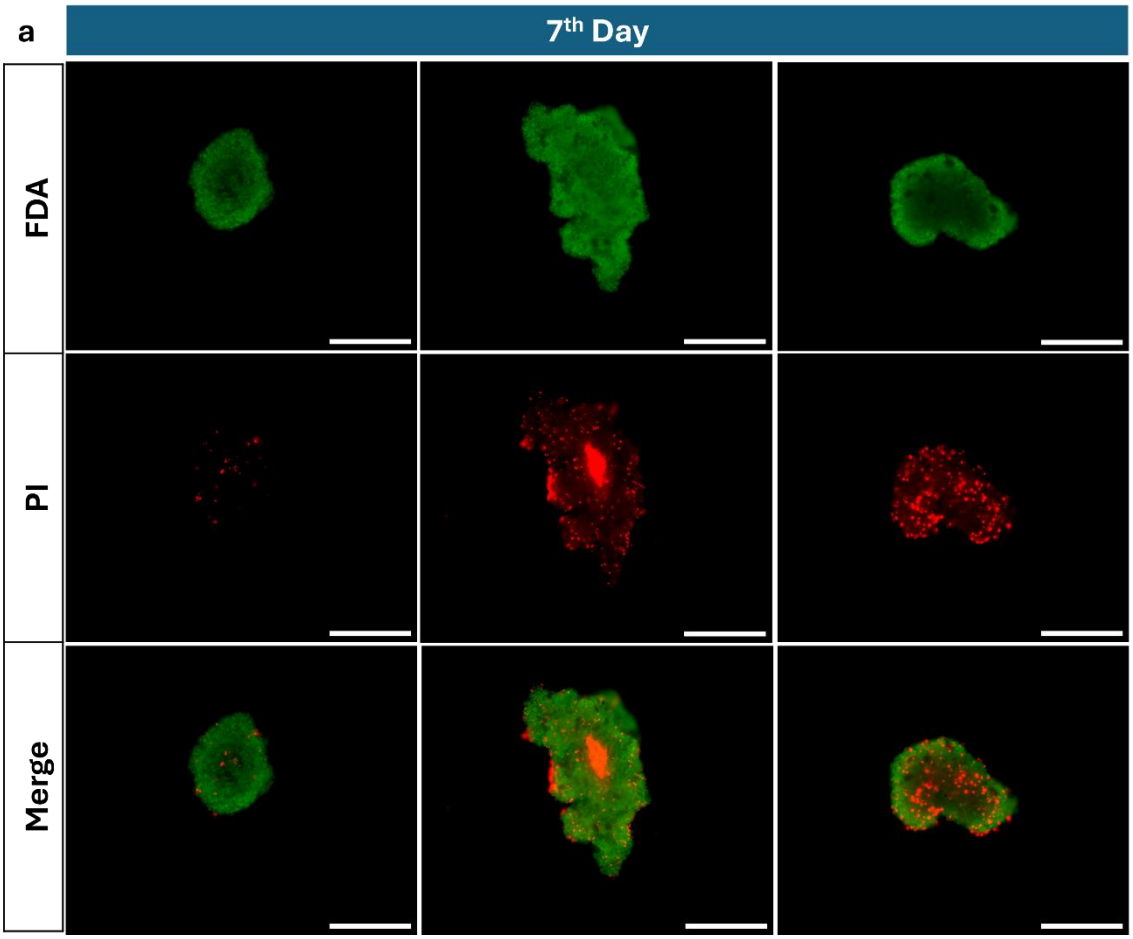

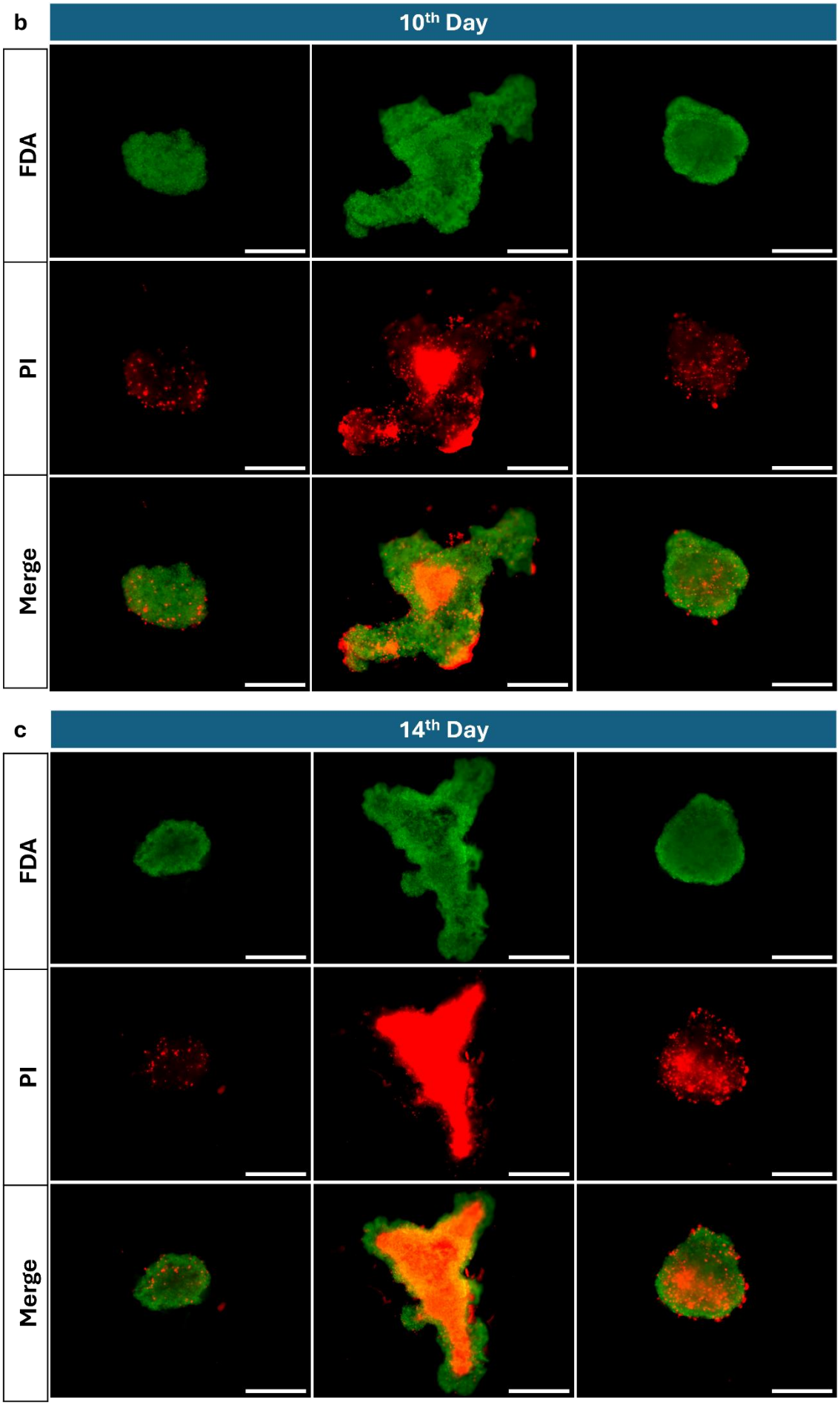

Figure 2.2.1 Live Dead results of U87-MG, SH-SY5Y and co-cultured spheroids with initial cell seeding density of 15000 cells on Day 7 (a), Day 10 (b), Day 14 (c). Scale 500 um

The live-dead assay works by the interaction dyes with the cellular components to represent live cells and dead cells with different fluorescence. In this case, the dyes used were Propidium Iodide (PI) and FDA (Fluorescein diacetate). PI permeates the dead cells and intercalates with their DNA. These cells, when excited with a particular wavelength result in red fluorescent emission indicating dead cells. On the other hand, though FDA doesn't have inherent fluorescent potential but when permeating live cells, the esterases in FDA are converted to Fluorescein, a green, fluorescent molecule.

Over the course of 14 days, the viability of U87-MG spheroids remained high while evidently SH-SY5Y spheroids viability decreased significantly. This could be attributed to the ability of U87-MG to grow well in hypoxia conditions[17] and there is no necrotic core formed yet as their sizes are still around 500µm. Studieshave reported that spheroids are more quiescent and hypoxic in this size range[15]. Also, hypoxia itself can create a necrotic core, and this tendency is seen in neuroblastoma spheroids. Right from Day 7, they have a necrotic core, and we can clearly see the size of the necrotic core increasing. By Day 14, almost the entire central region of the neuroblastoma spheroid has become necrotic. This indicates that, even in co-cultured spheroids, the neuroblastoma cells could be the ones which are necrotic.

2.3 DRUG TREATMENT

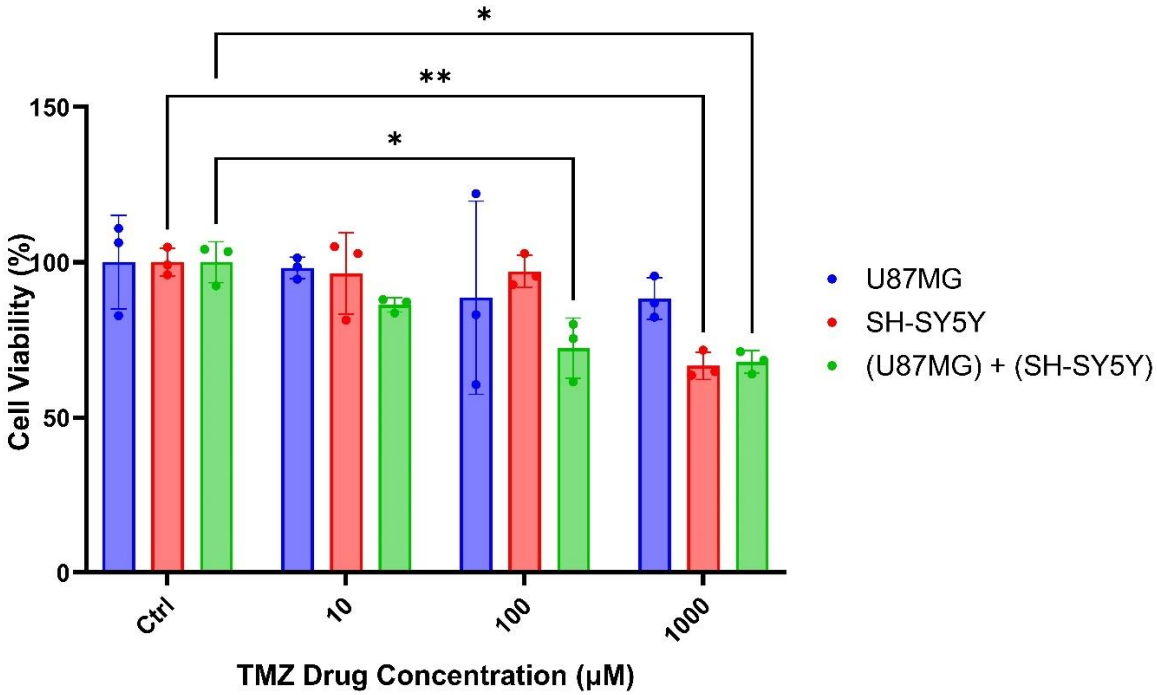

Figure 2.3.1 Cell Viability of the spheroids on Day 8 (after 24h DT on Day 7)

The CellTiter-Glo-3D assay quantifies the ATP activity of the viable cells in luminescent form. The luciferase enzyme promotes the oxidation of luciferin in the presenceof ATP generating luminescence. After 24h drug incubation, the cell viability results (Fig 2.3.1) asquantified with luminescence shows that U87MG spheroids were resistant to TMZ at all concentrations with minimal change. Even after 1000μM treatment, the cell viability remained around 88% while in case of SH-SY5Y spheroids and co-cultured spheroids, the % viabilities went down to ~67% and ~68% respectively at the same concentration level showing significant cancer reduction. Also, the viability results show that SH-SY5Y spheroids are sensitive only after 100uM concentration whereas the co-cultured spheroids are vulnerable to TMZ treatment at all the concentrations treated. The viability of co-cultured spheroids, decreased from 86% to 72% to 68% at concentrations 10, 100 and 1000μM. This clearly shows the effect of interplay between U87MG spheroids and SH-SY5Y spheroids when cultured together as compared to individual U87MG spheroids where they were resistant to the TMZ treatment and individual SH-SY5Y spheroids were more sensitive. And on co-culture, the spheroids are sensitive to treatment even at 10μM and consistently going down in % viability. The individual U87MG and SH-SY5Y groups are not sensitive to treatment at 10μM maintaining viabilities around ~97%. At 100μM U87MG was sensitive while SH-SY5Y still remained resistant. Then suddenly a significant decrease in viability was observed in SH-SY5Y spheroids at 1000μM.

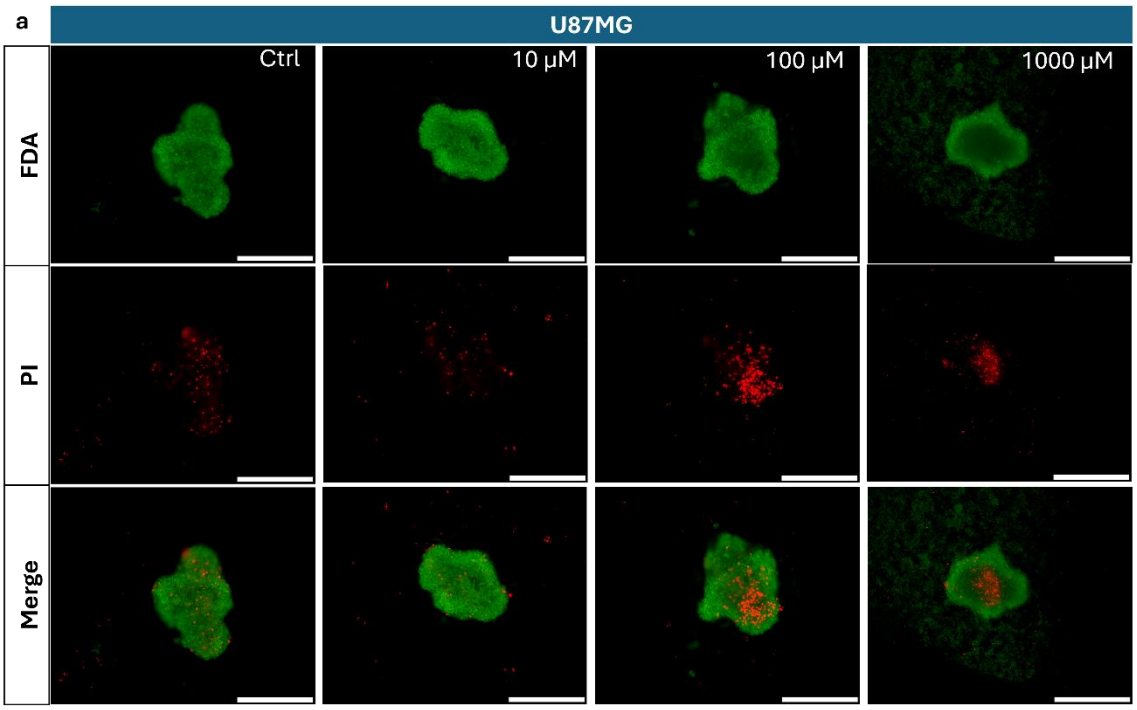

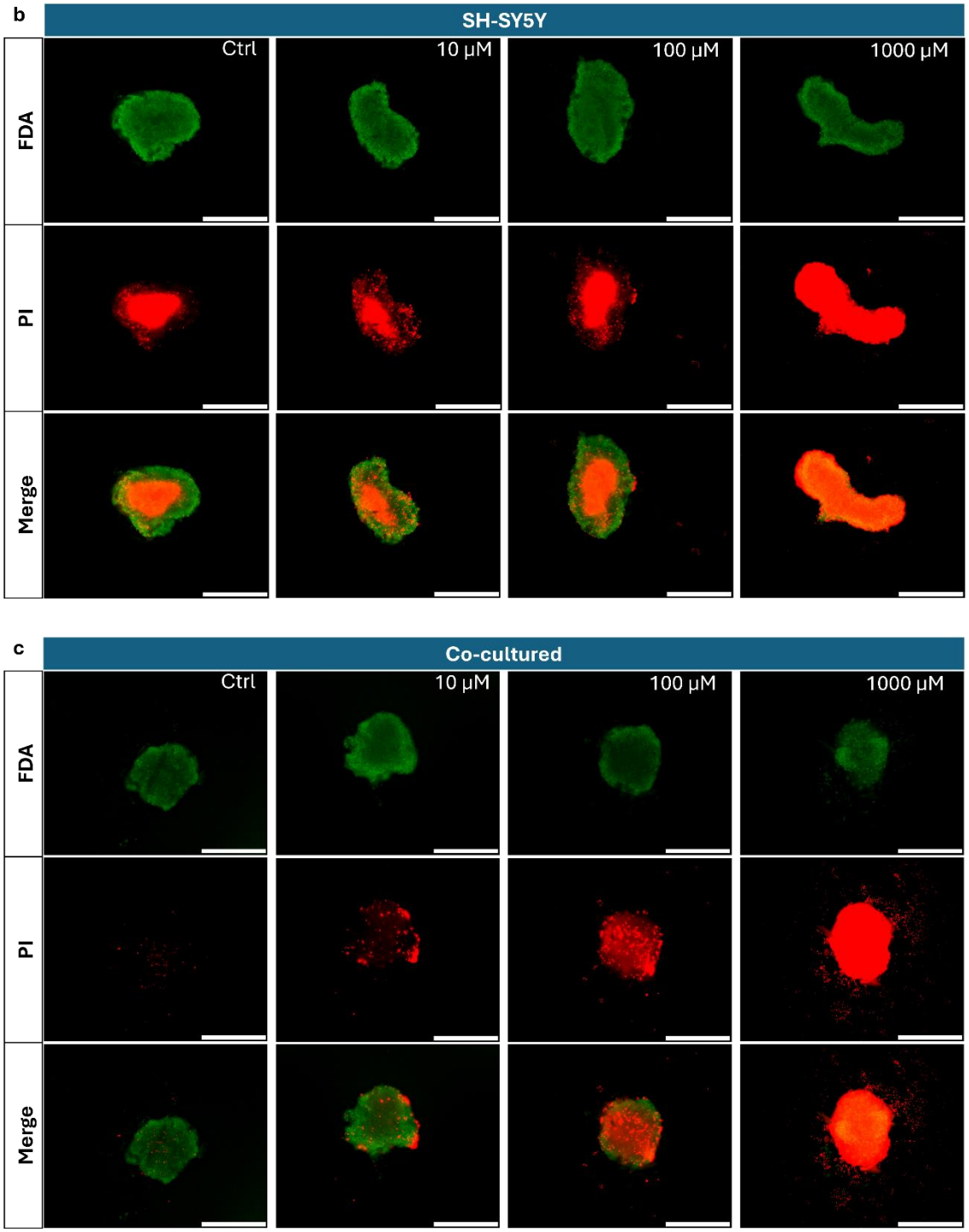

Figure 2.3.2 Live Dead Assay on the spheroids on Day 8 (after 24h DT on Day 7)

The live dead assay performed over TMZ treated spheroids reveal that the co-cultured spheroids at higher concentrations were able to kill the tumor. But when the SH-SY5Y spheroids are observed, is where the clarity that the tumor death on co-cultured spheroids is realized to be due to the influence of neuroblastoma and not due to glioblastoma. Though the live cells remain significantly high in glioma (Fig 2.3.2a), compared to Day 7 before drug treatment, the area on Day 8 after 24h drug treatment showed a decrease in size (Supplementary Figure S4, S5a). In individual

neuroblastoma spheroids (Fig 2.3.2b), increase in concentrations has led to cell death in the spheroid core which can be attributed to the necrotic core being susceptible to the drug easily. The areas observed there indicate a linear downward trend in proliferation with increasing concentration (Supplementary Figure S4, S5b). At 1000 μM the area remains almost the same both before and after drug treatment. For other concentrations and control, the amount of increase in area has decreased. In case of co-cultured spheroids, for control and 10μM there was a non-significant increase in area of spheroid and at 100 and 1000μM there was a non-significant decrease (Supplementary Figure S4, S5c). In live dead of co-cultured spheroids, cell death has started from the periphery and moves towards the center with the increase in concentration as observed in (Fig 2.3.4c) at 10μM and 100μM. In glioma spheroids at lower concentrations, the drug only disintegrated the cell debris from the outer proliferation zone. But at 1000μM, spheroids have dispersed as cellular aggregates but still they remained viable. For neuroblastoma spheroids, from Fig 2.2.1 we can see that they have a central necrotic core on Day 7 unlike the glioma and co-cultured spheroids. A similar pattern has been noticed even here in the control on Day 8. Lower concentrations (10μM and 100μM) on neuroblastoma spheroids-maintained cell viability closer to that of control but a logarithmic increase to 1000μM strongly decreased the cell viability. The live dead results of co-cultured spheroids indicated their high sensitivity to TMZ as cell viability decreased in linear manner with increase in dosage. Similar to glioma spheroids, at 1000μM co-cultured spheroids also showed a strong disaggregation of cells but here they stained red indicating cell death. Overall, these results exactly reflect the quantitative cell viability (ATP Assay) results of our work.

3 DISCUSSION

Numerous works have been published on the co-culture of astrocyte and neuronal cells. They are generally direct and indirect (transwell system, conditioned media) monolayer cultures. Though they add upon the available knowledge of astrocytes and neurons, they don't reciprocate *in vivo*. Also, some 3D co-culture works have been published by differentiating hiPSCs into neurons and astrocytes. In this case, the tumor microenvironment is missing to model for high grade cancers like glioblastoma.

SH-SY5Y and U87-MG mono-layered cells were co-cultured in a transwell setup using Irradiated cell conditioned medium (ICCM) to evaluate the indirect effects of

radiation on SH-SY5Y cells. The results from the work proposed that co-culture of U87MG glial cells may have alleviated oxidative stress, DNA damage and decreased apoptotic protein levels in SH-SY5Y neuronal cells[14]. This might hold true for our work as the live dead results of SH-SY5Y showed higher cell death compared to when they were co-cultured with U87-MG cells.

A similar work carried out by De Simone and team explored the neuroprotection on SH-SY5Y by D384 glial (astrocyte) cell line using a transwell co-culture system under different neurotoxicant treatment. The results revealed that cytotoxicity of the drugs decreased in co-culture compared to treatment with neurons alone indicating resistance of astrocytes[2]. An inverse mechanism was noticed in our study. When glial derived cell lines replaced primary astrocytes, neurons could not survive more than 13 days in cell-insert co-culture systems[9]. Also, in our work neuronal spheroids could not survive 14-day. A large PI-stained region (about ~90%) was seen on Day 14.

Recently, Batenburg et al have developed a 3D co-cultured system of the neuron-astrocyte from hiPSCs integrated with tau-aggregation to understand tauopathies. The astrocytes from the co-cultured 3D model exhibited bipolar and stellate morphologies usually not observed in 2D culture. Neurons especially neuronal cell bodies of neurons were found to be closely connected with astrocytes and synapses, implying a tripartite synapse formation. The ability of astrocytes to enwrap neurite and neuronal soma was observed as well.[15] This work's results were comparable to our co-culture where astrocytoma cell line (U87-MG) influenced neuronal (SH-SY5Y) cells enwrapping neurites to form a spheroid like U87-MG. Neurite elongation has been considered an important morphological marker in neuronal differentiation[18]

Studies have reported that multicellular organization of SH-SY5Y enhances the neuron specific markers. Also, they suggest differentiation of SH-SY5Y in 3D models without additional reagents unlike in monolayer cultures. Another work adds evidence that it could be due to the ECM substrate being used for the spheroid growth which influences neuronal differentiation. A study by De Simone et al modelled 3D tumor models of Astrocytes (D384) and Neurons (SH-SY5Y) revealed that astrocytes formed spherical spheroids while the neurons followed an elliptical or irregular phenotype. This was due to higher proliferation rate of astrocytes[19]. All this strongly supports our hypothesis that the SH-SY5Y could have differentiated and is reflective in our results[19–21].

Further, Rickner et al have come up with their Neuron-Astrocyte co-culture model termed "Asteroid" seeded with tau oligomers to study tauopathies. The hiPSC derived co-culture spheroid model indicated close localization near sites of neuronal damage and larger area compared to astrocyte spheroids[10]. Our co-cultured 3D model as well-developed spheroids with larger area compared to astrocytoma (U87-MG) group. Simao and colleagues obtained a 3D neuron- astrocyte network by differentiating NT2 cells. The network was exposed to acrylamide which showed preferential uptake by neuronal populations. It led to impaired synaptic activity due to glutamate accumulation[5]. TMZ showed preferential uptake in U87-MG and co-cultured spheroids. Complex networks where neurons and glial cells communicate were seen on the 14th day of co-culture. GFAP stain suggested the support of astrocytes to neuronal cells and Tuj-1 displayed that neural networks are denser in 3D than 2D cultures[16].

Many groups have developed mathematical models to understand and predict the growth kinetics of spheroids[22–26]. The results of our work as well aligned well with their findings. All three zones of the cellular spheroid, namely proliferative outer zone, quiescent intermediary zone and necrotic core zone were visible in all our three types of spheroids. The spheroids (Fig 2.2.2) clearly saw a contractile phase for the initial 4 days[27].

During the initial phase of spheroid formation, cell-cell adhesion forces dominate, pulling cells together into a compact cluster, causing the spheroid to shrink. As cells begin to proliferate, the increased cell concentration within the spheroid generates pressure that counteracts the adhesion forces. This balance prevents further shrinking and leads to steady growth. This phase continues until necrosis occurs, where the interplay between cell division (mitosis) and cell death (necrosis) determines the growth pattern[26] . The transient structure of a spheroid does not depend on its initial size, and the final structure can be independent of the seeding density[28]. So, the growth after initial 4 days followed a sigmoidal curve pattern with exponential growth between 4th and 7th day while 7th to 10th day saw a transient slow growth phase indicating movement to a saturation phase (10th to 14th day).

In the initial days when diameter was small necrosis was not observed but with increase in size necrosis region was formed and grew larger. A linear relationship was observed in viable cell numbers and spheroid diameter. This was notably seen through the live dead results on Day 7,10,14 where Glioblastoma and Co-cultured spheroids

which had a saturated size values maintained their cell viability while Neuroblastoma which increased in size showed increased cell death[29]. As per Aria and group, spheroids of glioblastoma and non-small cell lung cancer (NSCLC) were extremely compact, making it difficult to assess the amount of free space between neighbouring nuclei. They also displayed signs of cell crowding, which could have led to changes in cell size near the core. On the other hand, neuroblastoma spheroids maintained measurable and constant free space throughout the model, which was consistent with findings from their simulated low-density spheroids and our results[30].

Spheroids with sizes below 100µm and within 4 days of growth generally doesn't have any defined zone[17]. Similarly, only spheroids above 500µm showcase a necrotic zone which however might differ based on cell line. In our case, some spheroids above 500µm showed necrotic zone. But clearly with the increase in size, the probability of a necrotic zone and the necrotic zone's area increased. This is because the diffusion limit of oxygen is 150-200µm from the outer layer[13]. Furthermore, the hypoxia-inducible factor (HIF)-1α is stabilized at around 80µm inward from the proliferative zone. This suggests that all necrotic cores are hypoxic but not the other way around[18]. In U87-MG spheroids, a necrotic core was observed based on the grayscale intensity, but live dead results showed them completely viable demonstrating they were hypoxic. Similar results were obtained by Jingyun and team with glioma spheroids[31].
SH-SY5Y had a necrotic core as early as 7th day and U87-MG did not even have on 14th day. This suggests that necrosis occurs in a size dependent manner in spheroids than time dependent.

When the circularity of the spheroid was high, even diffusion was observed, the growth rate was low, and the response to the drug was high. This was not true to our case where Glioblastoma whose circularity was better than that of neuroblastoma was resistant to drug. At the same time, the co-cultured spheroids which also had good circularity showed a strong sensitivity to the drug. So, we find that it depends on the cell type and drug and can't be generalized[32].

Various studies with drug treatment of temozolomide (TMZ) in glioblastoma spheroids have been carried out. While U87-MG spheroids with sizes between 150-350µm responded to 100µM, the spheroids above 400µm did not. Our results suggest the same. All our spheroids were above 400µm, at 100µM there was not significant decrease in viability of any of our spheroid groups. Concentrations above 200µM have resulted in spheroid disaggregation in a 24h study while concentrations lesser than that ablated the spheroid surface[12]. As our studies were at logarithmic concentrations, the spheroid disaggregation pattern was observed at 1000µM and only in glioma and co-cultured spheroid groups. This mechanism of action of the drug and spheroid response has been reported by Anna et al[13]. TMZ showed a dose- dependent inhibition of cell growth in all groups but significant effects were seen only in neuroblastoma and co-cultured spheroids. Temozolomide has been reported to be more toxic to neurons than glial cells, strongly validating our results[22].

4 CONCLUSION

In this work we have come up with a co-cultured 3D tumor disease model to screen brain cancer drugs. We have focused mainly on morphological and visual cues of spheroid model developed and their control groups to know the efficacy of the drug. This simple straight forward methodology can be widely opted for drug screening. Our further work, however, will be towards learning the biochemical cues of the model as it will help in designing and developing targeted drugs for Brain cancer meanwhile enhancing the understanding on the disease.

5 METHODOLOGY

5.1 CELL CULTURE AND FORMATION OF SPHEROIDS

The glioblastoma and neuroblastoma cells were given by Prof. James Curtin (Technical University Dublin) and Prof. Dennis Barry (Trinity College Dublin) respectively. The cells were cultured in a DMEM media supplemented with 1% penicillin-streptomycin, 1% L-Glutamine (Merck Life Sciences) and 10% Fetal Bovine Serum (Cytiva HyClone). The Phosphate Buffer Saline (PBS) and Trypsin needed for the washing and detachment of cells were also obtained from Merck life sciences. The cells were maintained at 37°C and 5% CO_2.

Initially, Flat-bottomed 96 well plates (SPL Life Sciences) were coated with 1% agarose solution (Fisher Scientific). Then, cell suspensions with cell densities of 5000, 10000 and 15000 per well were prepared in 200µL medium for U87-MG and SH-SY5Y. Equal amount (100µL each) of U87-MG and SH-SY5Y cells were used to develop the co-cultured spheroid model. The spheroids were grown for 14 days. Media was changed on the 4th, 7th and 10th day after imaging. While changing media, only 100 µL of the old spent media was removed so as not to perturb the spheroids and dissociate them. Then new 100µL media was added gently on the walls of the well to minimize the stress on the spheroids. Phase contrast microscope images of the spheroids were taken each day using a Keyence BZ-X810 Microscope.

5.2 LIVE DEAD ASSAY

Live Dead Assay, a qualitative way of assessing the cell viability of spheroids was performed on 7th, 10th and 14th day. Briefly, 150 µL of media was removed from each well, washed with PBS and were added with 10µL of Propidium Iodide (PI) followed by Fluorescein Diacetate (FDA) dissolved in PBS and Acetone respectively. The concentration of dyes was kept constant at 0.5mg/mL. After an incubation period of 10min, the spheroids were washed twice with PBS and taken directly for fluorescence imaging using a Keyence BZ-X810 Microscope.

5.3 DRUG TREATMENT

The spheroids were treated with Temoside® formulation obtained from Cipla Ltd, India at a logarithmic range to know the efficacy range of the drug in spheroid models developed. The concentration was based on the amount of active pharmaceutical ingredient – Temozolomide. The final drug concentration was maintained at 10,100 and 1000μM.

ATP Assay:

On the 7th day of spheroid growth, 150μL spent medium was removed from the 200μL media in each well and 50μL of Drug dissolved media was added. After 24h, the spheroids were added with 100 μL of Cell-Titer Glo 3D®, incubated at room temperature for 30min. The luminescence values were obtained using BioTek Synergy H1 multimode plate reader.

Live Dead Assay:

On the 7th day of spheroid growth, 100μL spent medium was removed from the 200μL media in each well and 100μL of Drug dissolved media was added. On Day 8, the spent media was removed and washed with PBS. Incubated with PI and FDA and imaged.

5.4 STATISTICS

All image measurements were made using ImageJ. All statistical analyses in this work were performed using either Python or GraphPad Prism software version 10.2.0 (GraphPad Software, Inc., La Jolla, California, USA). Repeated measures Two-way ANOVA statistic method with post-hoc Tukey test was used. $P < 0.05$ was considered significant ($n = 3$).

Data statement

All data presented in this manuscript is available from the corresponding author on request.

Author Contributions

Conceptualization – NT, SM. Data Curation – NT, SM, AM. Formal Analysis – SM, AM. Funding Acquisition – NT. Methodology – SM. Project Administration – NT,TS. Resources – NT, TS. Software – AM. Supervision – NT. Validation – SM. Visualization – SM. Writing/Original Draft Preparation – SM. Writing/Review & Editing – SM, NT.

Acknowledgements

Authors acknowledge funding under the Science Foundation Ireland and Irish Research Council (SFI-IRC) pathway program (21/PATH-S/9634).

REFERENCES

1 R. Afridi, J.H. Kim, M.H. Rahman, and K. Suk, "Metabolic Regulation of Glial Phenotypes: Implications in Neuron–Glia Interactions and Neurological Disorders," Front Cell Neurosci 14, (2020).
2 U. De Simone, F. Caloni, L. Gribaldo, and T. Coccini, "Human Co-culture Model of Neurons and Astrocytes to Test Acute Cytotoxicity of Neurotoxic Compounds," Int J Toxicol 36(6), 463–477 (2017).
3 M. Bélanger, I. Allaman, and P.J. Magistretti, "Brain energy metabolism: Focus on Astrocyte-neuron metabolic cooperation," Cell Metab 14(6), 724–738 (2011).
4 Y. Pan, and M. Monje, "Neuron–Glial Interactions in Health and Brain Cancer," Adv Biol 6(9), (2022).
5 D. Simaõ, A.P. Terrasso, A.P. Teixeira, C. Brito, U. Sonnewald, and P.M. Alves, "Functional metabolic interactions of human neuron-astrocyte 3D in vitro networks," Sci Rep 6, (2016).
6 V. Chavda, K. Singh, V. Patel, M. Mishra, and A.K. Mishra, "Neuronal Glial Crosstalk: Specific and Shared Mechanisms in Alzheimer's Disease," Brain Sci 12(1), (2022).
7 Y. Iwadate, K. Fukuda, T. Matsutani, and N. Saeki, "Intrinsic protective mechanisms of the neuron-glia network against glioma invasion," Journal of Clinical Neuroscience 26, 19–25 (2016).
8 S. Robel, and H. Sontheimer, "Glia as drivers of abnormal neuronal activity," Nat Neurosci 19(1), 28–33 (2015).
9 M. Pyka, C. Busse, C. Seidenbecher, E.D. Gundelfinger, and A. Faissner, "Astrocytes are crucial for survival and maturation of embryonic hippocampal neurons in a neuron-glia cell-insert coculture assay," Synapse 65(1), 41–53 (2011).
10 H.D. Rickner, L. Jiang, R. Hong, N.K. O'Neill, C.A. Mojica, B.J. Snyder, L. Zhang, D. Shaw, M. Medalla, B. Wolozin, and C.S. Cheng, "Single cell transcriptomic profiling of tauopathy in a novel 3D neuron-astrocyte coculture model," (2022).
11 I.R. Calori, S.R. Alves, H. Bi, and A.C. Tedesco, "Type-I Collagen/Collagenase Modulates the 3D Structure and Behavior of Glioblastoma Spheroid Models," ACS Appl Bio Mater 5(2), 723–733 (2022).
12 I.R. Suhito, N. Angeline, K.H. Lee, H. Kim, C.G. Park, Z. Luo, and T.H. Kim, "A Spheroid-Forming Hybrid Gold Nanostructure Platform That Electrochemically Detects Anticancer Effects of Curcumin in a Multicellular Brain Cancer Model," Small 17(15), (2021).
13 A. Senrung, S. Lalwani, D. Janjua, T. Tripathi, J. Kaur, N. Ghuratia, N. Aggarwal, A. Chhokar, J. Yadav, A. Chaudhary, U. Joshi, and A.C. Bharti, "3D tumor spheroids: morphological alterations a yardstick to anti-cancer drug response," In Vitro Models 2(6), 219–248 (2023).
14 S.Y. Park, H.J. Hong, and H.J. Lee, "Fabrication of Cell Spheroids for 3D Cell Culture and Biomedical Applications," Biochip J 17(1), 24–43 (2023).
15 S. Däster, N. Amatruda, D. Calabrese, R. Ivanek, E. Turrini, R.A. Droeser, P. Zajac, C. Fimognari, G.C. Spagnoli, G. Iezzi, V. Mele, and M.G. Muraro, *Induction of Hypoxia and Necrosis in Multicellular Tumor Spheroids Is Associated with Resistance to Chemotherapy Treatment* (2016).
16 S.L. Valles, S.K. Singh, J. Campos-Campos, C. Colmena, I. Campo-Palacio, K. Alvarez-Gamez, O. Caballero, and A. Jorda, "Functions of Astrocytes under Normal Conditions and after a Brain Disease," Int J Mol Sci 24(9), (2023).
17 W. Huang, X. Ding, H. Ye, J. Wang, J. Shao, and T. Huang, "Hypoxia enhances the migration and invasion of human glioblastoma U87 cells through PI3K/Akt/mTOR/HIF-1α pathway," Neuroreport 29(18), 1578–1585 (2018).

18 V. De Conto, V. Cheung, G. Maubon, Z. Souguir, N. Maubon, E. Vandenhaute, and V. Bérézowski, "In vitro differentiation modifies the neurotoxic response of SH-SY5Y cells," Toxicology in Vitro 77, (2021).
19 G.S. Jung, K.M. Lee, J.K. Park, S.K. Choi, and W.B. Jeon, "Morphogenetic and neuronal characterization of human neuroblastoma multicellular spheroids cultured under undifferentiated and all-trans-retinoic acid-differentiated conditions," BMB Rep 46(5), 276–281 (2013).
20 D. Krinke, H.G. Jahnke, T.G.A. Mack, A. Hirche, F. Striggow, and A.A. Robitzki, "A novel organotypic tauopathy model on a new microcavity chip for bioelectronic label-free and real time monitoring," Biosens Bioelectron 26(1), 162–168 (2010).
21 G.N. Li, L.L. Livi, C.M. Gourd, E.S. Deweerd, and D. Hoffman-Kim, "Genomic and morphological changes of neuroblastoma cells in response to three-dimensional matrices," Tissue Eng 13(5), 1035–1047 (2007).
22 K.C. Iarosz, F.S. Borges, A.M. Batista, M.S. Baptista, R.A.N. Siqueira, R.L. Viana, and S.R. Lopes, "Mathematical model of brain tumour with glia-neuron interactions and chemotherapy treatment," J Theor Biol 368, 113–121 (2015).
23 A.M. Stein, T. Demuth, D. Mobley, M. Berens, and L.M. Sander, "A mathematical model of glioblastoma tumor spheroid invasion in a three-dimensional in vitro experiment," Biophys J 92(1), 356–365 (2007).
24 J. Bachmann, A. Raue, M. Schilling, V. Becker, J. Timmer, and U. Klingmu, "Predictive mathematical models of cancer signalling pathways ¨," 155–165 (2011).
25 C. Morabito, N. Steimberg, G. Mazzoleni, S. Guarnieri, G. Fanò-Illic, and M.A. Mariggiò, "RCCS bioreactor-based modelled microgravity induces significant changes on in vitro 3D neuroglial cell cultures," Biomed Res Int 2015, (2015).
26 M. Amereh, R. Edwards, M. Akbari, and B. Nadler, "In-silico modeling of tumor spheroid formation and growth," Micromachines (Basel) 12(7), (2021).
27 A. Carrasco-Mantis, H. Castro-Abril, T. Randelovic, I. Ochoa, M. Doblaré, and J.A. Sanz-Herrera, "A mechanobiological model for tumor spheroids evolution: application to glioblastoma," (2021).
28 A.P. Browning, J.A. Sharp, R.J. Murphy, G. Gunasingh, B. Lawson, K. Burrage, N.K. Haass, and M.J. Simpson, "Quantitative analysis of tumour spheroid structure," Elife 10, (2021).
29 W. Shi, J. Kwon, Y. Huang, J. Tan, C.G. Uhl, R. He, C. Zhou, and Y. Liu, "Facile Tumor Spheroids Formation in Large Quantity with Controllable Size and High Uniformity," Sci Rep 8(1), (2018).
30 A. Ahmed-Cox, E. Pandzic, S.T. Johnston, C. Heu, J. McGhee, F.M. Mansfeld, E.J. Crampin, T.P. Davis, R.M. Whan, and M. Kavallaris, "Spatio-temporal analysis of nanoparticles in live tumor spheroids impacted by cell origin and density," Journal of Controlled Release 341, 661–675 (2022).
31 J. Ma, X. Zhang, Y. Liu, H. Yu, L. Liu, Y. Shi, Y. Li, and J. Qin, "Patterning hypoxic multicellular spheroids in a 3D matrix - a promising method for anti-tumor drug screening," Biotechnol J 11(1), 127–134 (2016).
32 S.Y. Park, H.J. Hong, and H.J. Lee, "Fabrication of Cell Spheroids for 3D Cell Culture and Biomedical Applications," Biochip J 17(1), 24–43 (2023).
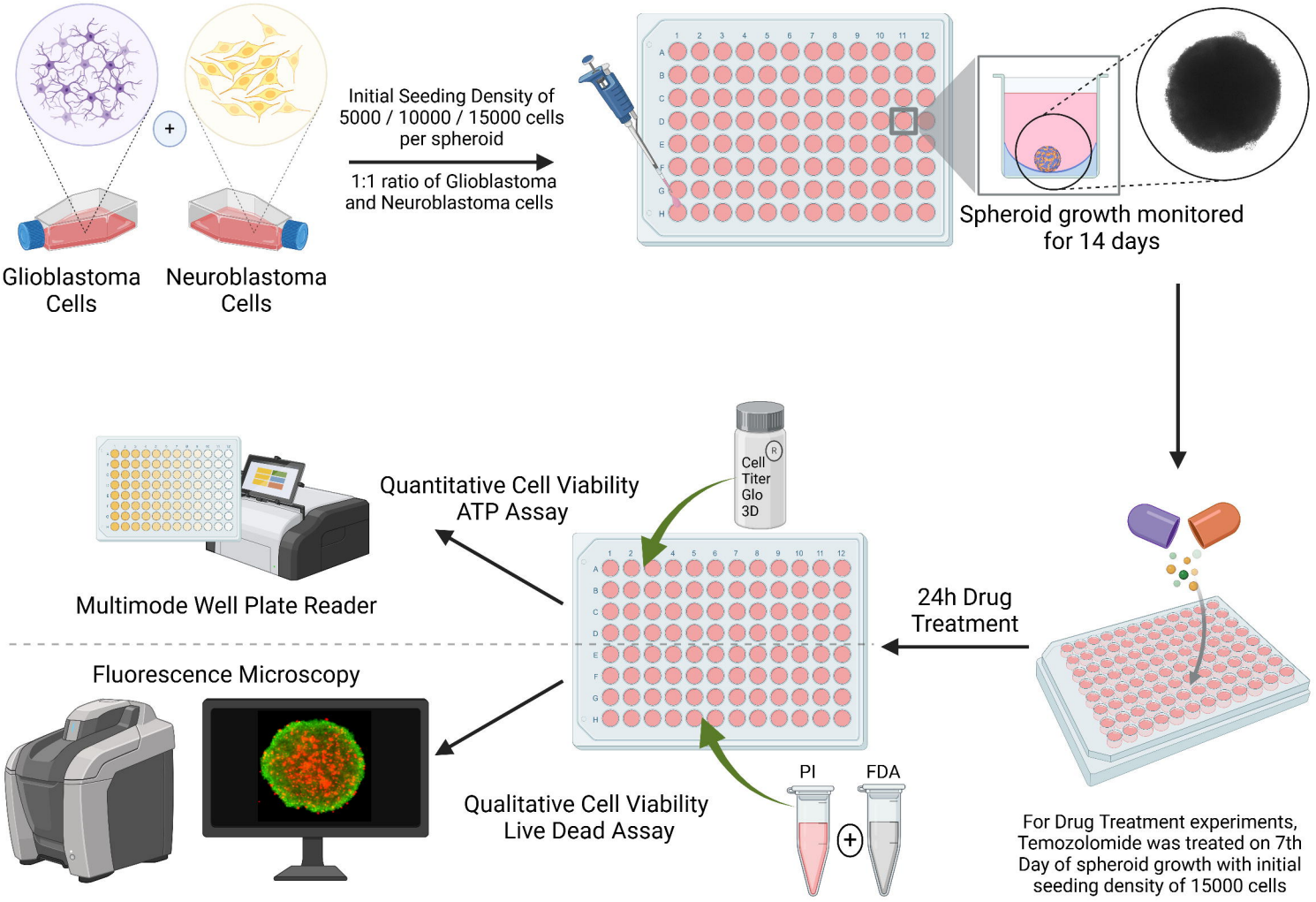
Multi-Cellular Tumor Spheroids (MCTS) for Brain Cancer Drug Screening